CrossMark

# High-resolution quantitative reconstruction of Late Cretaceous-Tertiary erosion in the West Netherlands Basin using multi-formation compaction trends and seismic data: implications for geothermal exploration

**Geza Worum[1] · Jan-Diederik van Wees[2,3]** (iD)

**Abstract** A workflow is presented to determine the detailed, high-resolution pattern of erosion in maturely explored Sedimentary Basins by analysing the sonic log-based interval velocity patterns of nine stratigraphic intervals complemented by a geometrical approach involving the extrapolation of 3-D seismic reflectors. The jointly evaluated results of the two approaches not only provide important constraints on the inversion tectonics of a basin, but are also used to better constrain its maturity history and reservoir quality for geothermal energy. The developed workflow is demonstrated for the West Netherlands Basin. The pattern of erosion, which is consistent with observed subcrop maps, shows increasing amount of erosion towards the East and reflects the complex deformation of the basin, in which the reactivation of faults played a major role. Indirectly the results also indicate that continuous, syn-inversion sedimentation was taking place on the flanks of the basin during the Late Cretaceous, while its centre was characterised by non-deposition or slight erosion. For geothermal exploration the inferred variations of amount of erosion has implications for the spatial distribution of porosity which is an important parameter for the assessment of reservoir quality.

**Keywords** Basin analysis · Sonic velocity · Geothermal

## 1 Introduction

The amount of erosion in a sedimentary basin is a vital parameter in basin analysis and in hydrocarbon geological studies. It has important control on the burial-, porosity- and diagenetic history of the reservoir rocks as well as on the thermal maturation of organic

✉ Jan-Diederik van Wees
jan_diederik.vanwees@tno.nl; jdanke@gmail.com

Geza Worum
worg@geomega.hu

[1] Geomega Ltd., Mester u. 4, Budapest 1095, Hungary

[2] Department of Earth Sciences, Universiteit Utrecht, Budapestlaan 6, Utrecht, The Netherlands

[3] TNO-Energy, Princetonlaan 6, 3508 TA Utrecht, The Netherlands

material and timing of hydrocarbon expulsion. In inverted sedimentary basins where complex deformation has occurred, laterally the amount of erosion may vary significantly. In such basins it is crucial to know not only the amount, but also the detailed pattern of erosion, since it provides important constraints on the style of inversion tectonics or on the fluid-flow system during inversion (e.g., Nalpas et al. 1995; Verweij 2003; Bouw and Oude Essink 2003).

There are several methods that aim to quantify the amount of removed sediments (for discussion on these methods see Skagen 1992; Nyland et al. 1992; Japsen and Chalmers 2000; Corcoran and Doré 2005). Analysis of the compaction trends of shales for example is a widely used method and has a potential accuracy of ±200 m (e.g., Nyland et al. 1992; Richardsen et al. 1993; Hansen 1996). Shales are ideal for the analysis because their porosity (and related physical properties i.e., sonic velocity, bulk density) shows a clearly depth-controlled trend, provided that during and/or after deposition overpressure did not developed in the succession. Other studies have demonstrated however, that beside shales, sandstones, mixed sediments and carbonates could also be used for this purpose (e.g., Bulat and Stoker 1987; Hillis 1991, 1993; Hillis et al. 1994; Japsen 1998, 2000). Time–temperature index-based (TTI) maturity modeling of organic material (e.g., Mathiesen et al. 2000) or EASYRo % method (Sweeney and Burnham 1990) can also provide constraints on the magnitude of erosion. However, the accuracy in this regard is low, since a wide range of input parameter combinations can provide the same "best fit" to the measured maturity indicators. As with maturity modelling, the temperature history of a sample revealed by fission track modelling is also affected by both the burial/exhumation of the sample and by the heat flow history (e.g., Green et al. 1989; Andriessen 1995). Although the accuracy of the estimated exhumation is less than that of the shale compaction analysis ($\sim$500–1000 m; Skagen 1992), fission track modelling is an extensively used method for erosion estimation, since it provides constraints also on the timing of the event (e.g., Rohrman et al. 1995; Mathiesen et al. 2000).

In this paper a multidisciplinary approach is presented aiming to quantify the detailed pattern of erosion in the West Netherlands Basin (WNB). The WNB was chosen as case study for the analysis, because in this basin large amount of publicly available exploration data is available (provided by TNO-NITG, National Geological Survey), which—by combining various methods—enables high resolution and accurate erosion reconstruction. The WNB is one of the major tectonic features of the Netherlands, which came into existence during the Mesozoic (e.g., Van Wijhe 1987; Ziegler 1990; Dronkers and Mrozek 1991; Racero-Baena and Drake 1996; De Jager et al. 1996; Worum et al. 2004; de Jager 2007). In the Late Cretaceous-Eocene period compressional stresses originating from the Alpine orogen inverted the basin in multiple stages (Late Cretaceous, Mid Paleocene and latest Eocene), which resulted in the complex deformation and deep erosion of the basin fill (Fig. 1). The erosion, which is marked by a significant hiatus across the basin, affected sediments from Eocene–Oligocene to Cretaceous, or even down to mid-Jurassic levels (Fig. 1). Quantitative reconstruction of the erosion has not been performed in the WNB before, and only indirect data are published with respect to erosion quantification (e.g., Bodenhausen and Ott 1981). It has to be emphasized, however, that the amount of erosion is expected to be laterally highly variable, since reverse reactivation of pre-existing faults played a major role during inversion (e.g., Racero-Baena and Drake 1996).

The workflow presented in this paper combines different approaches in order to provide a better-constrained erosion pattern in the WNB. The bulk of the erosion estimation comes from a compaction trend (or burial anomaly) analysis of nine, carefully defined lithostratigraphic units from six Jurassic-Cretaceous formations. In the present paper first the
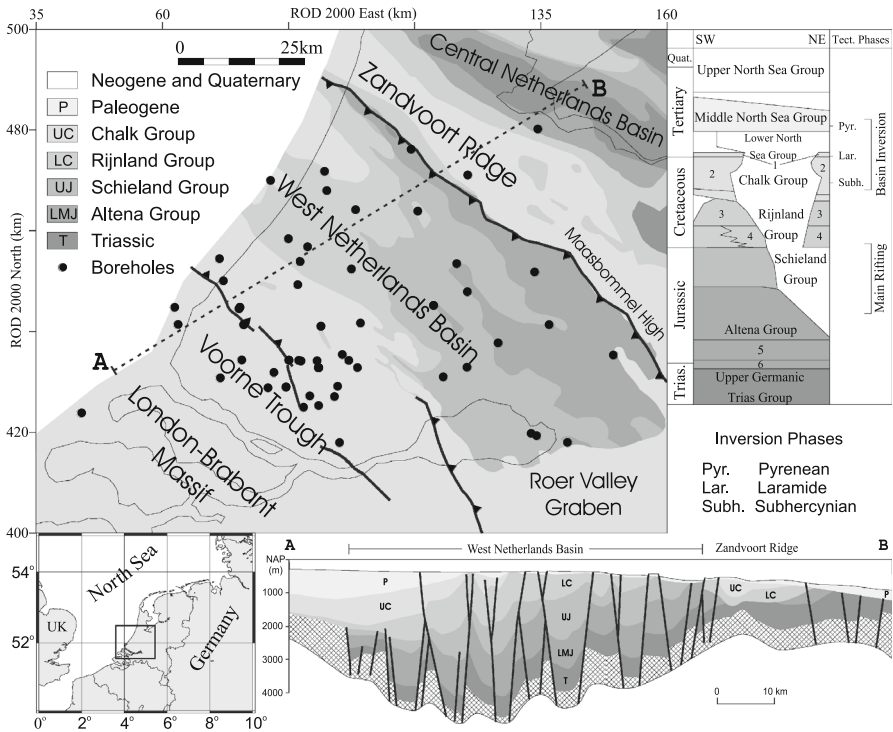
**Fig. 1** Pre-tertiary geological map, geological cross section and simplified litho-chronostratigraphical chart of the onshore West Netherlands Basin and surrounding areas. Boreholes used in the present study and the investigated formations are indicated. *1* Houthem Fm., *2* Ommelanden Fm., *3* Holland Fm., *4* Vlieland Claystone Fm., *5* Aalburg Fm., *6* Sleen Fm

principles of this method are discussed, with special emphasis put on its reliability and modified implementation, which is followed by the presentation of the results. The results provided by the burial anomaly analysis are complemented by those of other methods such as a statistical analysis of thickness data and a novel geometrical approach involving the analysis of 3-D seismic reflectors. In this regard the presented workflow is new, which—compared to other, standalone methods—allows a more accurate, high-resolution determination of the pattern of erosion in the basin. The results are evaluated jointly, which allows of the determination of the detailed pattern of erosion and the quantitative reconstruction of basin inversion in the WNB. The compiled map of erosion provides better constraints on the Late Cretaceous-Eocene tectonic. It affects the maturity history of the basin and the spatial distribution of the geothermal reservoir quality. These are discussed briefly at the end of the paper.

## 1.1 Burial anomaly analysis: methodology

The principle behind the analysis applied in this paper is the observation that average seismic velocity of a stratigraphic interval revealed by seismic surveys (e.g., Richardsen et al. 1993) or by sonic well-logs (e.g., Bulat and Stoker 1987; Hillis 1991, 1993; Hillis et al. 1994; Japsen 1998, 2000; Japsen et al. 2007) follows an increasing trend with depth.

The velocity-increase is caused by compaction and is assumed to be irreversible. Consequently, uplifted layers that are closer to the surface due to an erosional phase have higher sonic velocities than those that followed an uninterrupted subsidence path (Fig. 2). Comparison of the measured interval velocity with the normal depth-trend (also called "baseline") enables one to estimate the amount of erosion. The displacement, along the depth axis, of the measured interval velocity from the normal-depth trend is called the burial anomaly ($BA$) or apparent erosion (Fig. 2; Hillis 1993; Japsen 1998). It is zero for normally compacted sediments. Using the present-day depth of the studied interval ($D_p$) and the amount of post-erosional sediment thickness ($T_{pe}$) the amount of erosion ($E$) and the maximum depth of burial ($D_{max}$) can be calculated (e.g., Hillis 1993):

$$D_{max} = BA + D_p$$
$$E = BA + T_{pe} \tag{1}$$

Note that erosion estimation with this method is not possible if $T_{pe} > E$, since in this case the burial anomaly is destroyed (Fig. 2).

## 1.2 Implementation and reliability of the method

In the following the implementation and those modifications of the method are discussed, which were applied in the present paper in order to increase the reliability and the accuracy of the erosion estimation. The reliability of the burial anomaly analysis can be most easily increased if more than one interval is investigated at the same location. Namely, if no significant erosion occurred between the deposition of the units burial anomalies resulting
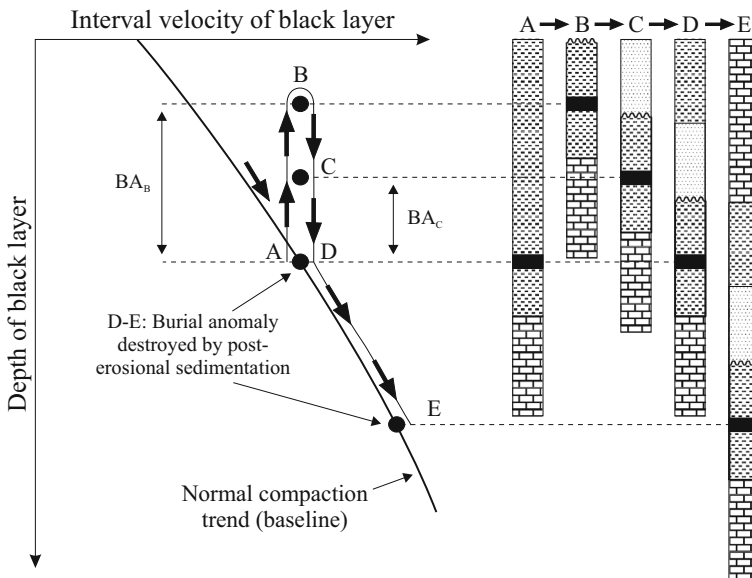


**Fig. 2** The evolution of interval velocity with burial/erosion. The interval velocity of a horizon (e.g., *black layer*) in an eroded sequence remains anomalous until the amount of post-erosional sedimentation reaches and exceeds the amount of erosion

from a young erosional episode should be equal (Japsen 2000). Should this be the case the estimation of erosion at the given location is more reliable.

The accuracy of the erosion estimates using burial anomalies depends on three factors: (1) the validity of the basic assumption (i.e., lithology and porosity are the primary controlling factors of the sonic velocity); (2) the type of stratigraphic interval chosen for the analysis and (3) the way the baseline is defined.

Although sonic velocity depends primarily on the lithological composition and the porosity of the sample (e.g., Vernik and Nur 1992; Japsen 1993; Kenter et al. 1997), other internal and external factors may be also important. For example, diagenetic differences between two samples having the same porosity and lithology often result in different sonic velocities, especially in carbonate rocks (Anselmetti and Eberli 1993; Kenter et al. 1997; Mallon and Swarbrick 2002; Fabricius 2003). Effective stress variations caused by pore fluid pressure fluctuations also have impact on the sonic velocity (Anselmetti and Eberli 1993; Japsen 1994, 1999, 2000; Kenter et al. 1997; Poix 1998). Furthermore, Moos and Zoback (1983) and Monsen (2001) demonstrated that the presence of microfractures can also significantly influence (reduce) sonic velocity. In light of these results during interpretation of anomalous interval velocities in this paper we used all available information (e.g., borehole- and pressure conditions, local geological and sedimentological circumstances revealed by well logs) to identify and ignore such anomalies, which were suspected to be the results of factors other than compaction and exhumation.

The second factor controlling the accuracy of the estimated erosion is the type and characteristics of the investigated stratigraphic interval. Interval velocities are generally calculated for lithostratigraphic groups or formations deposited in an open-water environment, since they can be easily recognized and correlated over large distances (e.g., Bulat and Stoker 1987; Hillis 1991, 1993; Hillis et al. 1994; Japsen 1998, 2000). Continental or near-shore deposits are not ideal for the analysis, since rapid lateral facies- and lithological changes often characterize them. This could result in a misleading interpretation of the burial anomalies. Through a thick stratigraphic unit such as a formation or group, however, lithology and consequently the sonic velocity pattern, is rarely uniform. This could also lead to misinterpreted (i.e., lithology-rather than erosion-related) burial anomalies, in cases when the formation is not complete. It is proposed therefore that the interval velocities should be calculated using thinner intervals, in which the lithological and sedimentological circumstances are more uniform. Wireline log patterns—if available—are ideal to define those intervals. The log pattern would also make it possible to reliably correlate the selected intervals over the study area. Using this approach the impact of lateral and vertical lithological/sedimentological variations on the burial anomalies and on the erosion estimates can be minimized.

The third crucial factor in the burial anomaly analysis is the definition of the baseline (i.e., normal compaction trend), since it has great impact on the amount of estimated erosion. In case of a lithologically pure formation (e.g., shale, chalk) published baselines can be used, which have been determined for the given lithology (e.g., Nyland et al. 1992; Japsen 1998, 1999). These baselines are often based on data from different basins and are represented by one or more analytical formulas (e.g., Magara 1976; Heasler and Kharitonova 1996; Japsen 1998). Other authors (Bulat and Stoker 1987; Hillis 1993; Hillis et al. 1994) used baselines fitting to the lowest interval velocity values observed in the given region. Such baselines overestimate the erosion and provide only rough estimates. To minimize baseline-related errors we propose that, when regional geology and available data allows it, baselines should be determined from those wells of the study area (referred to as reference wells/points), where no erosion is expected, or where the effect of erosion is

overprinted by the post-erosional sedimentation. This way of baseline definition provides the most accurate erosion estimates, since regional sedimentological and lithological circumstances affecting the sonic velocities are incorporated into the baseline and are taken into account. It is to be emphasized that in an ideal case the reference points should align along a smooth, quasi linear trend. A "noisy" reference data set suggests that not uniform lithology/diagenesis, borehole conditions or post-depositional impacts such as overpressure or hydrocarbons rather than extent of erosion are affecting the signal. In these cases the general reliability of the estimated erosion should be considered being lower. As the reference points never align perfectly along a trend, only those deviations that are clearly separated from the cloud of reference points are considered to be true anomalies.

## 2 Burial anomaly analysis: application to the West Netherlands Basin

Below, the interval velocity analysis of nine stratigraphic units from six Jurassic-Cretaceous formations are presented. The analyzed formations belong to the Late Cretaceous Chalk Group (Houthem and Ommelanden Fm.), the Early Cretaceous Rijnland Group (Holland and Vlieland Claystone Fm.) and the Early Jurassic Altena Group (Aalburg and Sleen Fm.) (Figure 1; Van Adrichem Boogaert and Kouwe 1997). Following the principles discussed above thin subintervals rather than complete sequences were used for the analysis. These intervals have thickness up to ~100–150 m and correspond to well sections of uniform log characteristics. In some cases the log pattern of the formations made it possible to reliably correlate these intervals across the basin.

The average sonic velocities of the selected intervals were calculated using the integrated travel time (ITT) derived from sonic well-logs and the thickness of the interval. In cases where the ITT peaks were not displayed along the sonic log, manually averaged slowness values were obtained, which later were converted into interval velocity. The true vertical depth of the midpoint of the interval represents the reference depth for every interval velocity value.

On the southern flank of the WNB only a small amount of Late Cretaceous erosion occurred, which was followed by significant Tertiary subsidence (Fig. 1; Voorne Trough). In this part of the basin Mesozoic sediments presently are buried to their maximum (i.e., any erosion-related burial anomaly is destroyed by the Cenozoic sedimentation). Therefore, interval velocity data from wells located in this part of the basin (referred to as reference wells/points) are used to constrain the normal depth trends.

### 2.1 Chalk (Houthem and Ommelanden formations)

As demonstrated by Anselmetti and Eberli (1993) sonic velocity of limestones depends on the porosity and diagenesis of the rock rather than on its depth, which make them less ideal for the burial anomaly analysis. Chalks however, though chemically identical to limestones, usually show a clearly depth controlled compaction trend (e.g., Mallon and Swarbrick 2002; Fabricius 2003), which makes them suitable for this kind of analysis (Hillis 1991; Japsen 1998). It should be noted however, that syn-sedimentary features such as chalk slumps are often associated with zones of significant overpressure and anomalous porosity/sonic velocity. The early entry of hydrocarbons into the pore space of these zones—which form excellent reservoirs in the North Sea region—can further enhance the porosity anomaly (e.g., Cornford 1994).

Within the Late Cretaceous-Early Paleocene Chalk Group, which is preserved only on the flanks of the basin (Fig. 3b), three intervals were investigated: two intervals from the Ommelanden Formation (referred to as Lower- and Upper Chalk interval, respectively) and a ~20 m thin interval from the Houthem Formation (referred to as Houthem Chalk). These intervals were defined and correlated using wireline log patterns in 32 wells (Fig. 3a). It is important to note that the deposition of the chalk in the WNB is coeval with the early phases of basin inversion and that the lowest interval pre-dates, while the upper intervals post-date the Late Santonian-Mid Campanian inversion phase. Probably this is the reason why the syn-inversion chalk interval between them has a non-uniform sonic- and resistivity-log response (syn-tectonic features?), which makes the correlation of this interval over large distances not possible.

The interval velocity-depth pairs for the three chalk intervals are shown in Fig. 3c, d. The log suites of six wells contain not only sonic- but also density logs, which made it possible to calculate average bulk densities for the Lower Chalk interval. Using the average density versus sonic velocity plot a conversion formula was calculated, which was
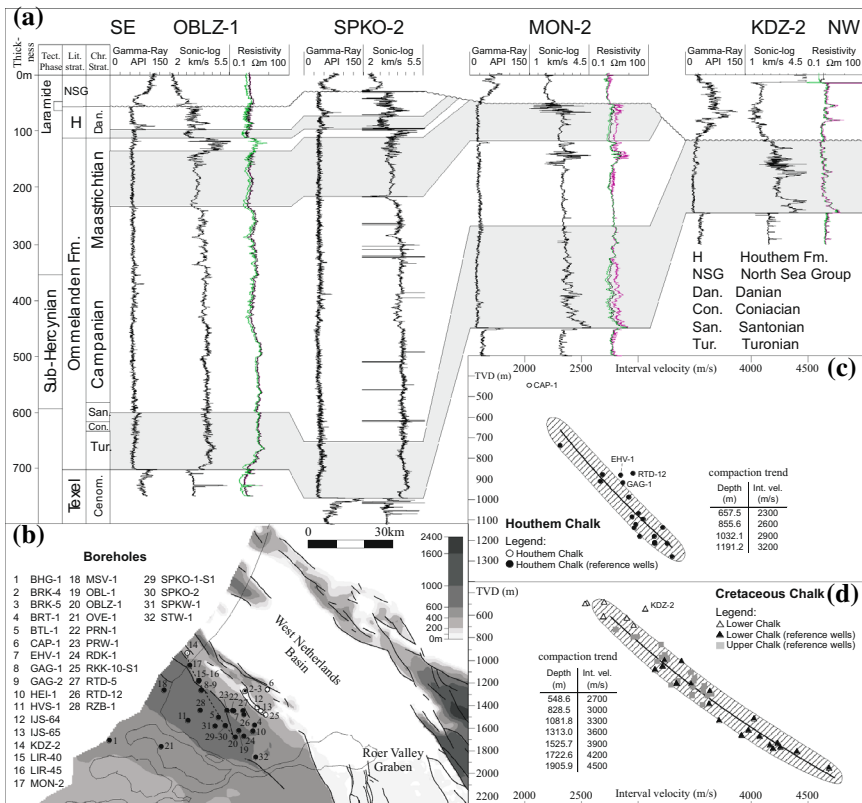


**Fig. 3** **a** Litho-chronostratigraphy and characteristic log pattern of the Chalk Group. The investigated intervals (Lower-, Upper and Houthem Chalk) are indicated in *grey*. **b** Preserved thickness of the Chalk Group. Boreholes indicated by *black circles* represent the reference wells that were used to constrain the baselines. **c** Interval velocity-depth pairs for the Houthem Chalk interval. **d** Interval velocity-depth pairs for the Lower and Upper Chalk intervals

used to convert the measured average bulk density of wells RKK-10-S1 and IJS-65 into a sonic velocity. In these wells sonic velocity data are not available.

### 2.1.1 Houthem chalk

Except for three data points (EHV-1, GAG-1 and RTD-12) the reference velocity-depth pairs of the Houthem Chalk (Fig. 3c) follow a quasi-linear trend. The observed anomalies are not erosion-related, since in these wells minor erosion is thought to have taken place and the post-chalk sedimentation is significant. It is important to note that well CAP-1 also fits into the trend, although has only 86 m of preserved chalk, suggesting that the burial anomaly signal is masked by the Cenozoic subsidence.

### 2.1.2 Lower and upper chalk intervals

The interval velocity of the Lower and the Upper Chalk intervals for the reference wells behaves similarly with depth (Fig. 3d). The trends align along a clean line, which represents the baseline. Data points shallower than $\sim 700$ m belong to wells that are located along the axis of an uplifted/folded half-graben (only 50–100 m of preserved chalk). In these wells (CAP-1, BRK-4, BRK-5, IJS-64, IJS-65, RKK-10-S1; marked by open circles on Fig. 3b) a certain amount of burial anomaly would be expected, but none was found, suggesting that presently the Cretaceous chalk in these wells is buried at its maximum. In case of well KDZ-2–250 m of burial anomaly is observed. Considering that this well has similar tectonic position and preserved chalk thickness than the wells mentioned above, it is unlikely that this anomaly is erosion-related. A clear explanation for this anomaly has not yet been found.

### 2.1.3 Comparison with published baselines

The uniform lithology of the chalk makes it possible to compare the results of this study with compaction trend lines obtained from other Cretaceous– or present day oceanic basins (Fig. 4; Scholle 1977; Sclater and Christie 1980; Japsen 2000; Mallon and Swarbrick 2002). In order to convert the porosity-depth baselines of Scholle (1977) and Sclater and Christie (1980) into sonic velocity-depth lines the conversion formula of Japsen (1998) and of Mallon and Swarbrick (2002) were used.

Comparison of the various baselines reveals that the impact of the porosity-sonic velocity conversion formulas on the resulting baselines is significant. The baseline of Mallon and Swarbrick (2002) is based on interval velocity measurements of non-reservoir North Sea chalk as well as carefully selected DSDP wells, in which the composition of the sediments is comparable with that of the chalk in the WNB. Above 1000 m this curve as wells as the porosity-depth curves converted by Mallon and Swarbrick's (2002) formula fit particularly good with the data presented in this study. The curve of Japsen's (2000) and the porosity-depth curves converted by Japsen's (1998) formula seems to fit better to the Houthem Chalk at shallow depth. At greater depth, almost all of the curves fit reasonably well taking into account the estimated accuracy of the method (±200 m Skagen 1992).

To summarise, it is concluded that the baseline determined for the Cretaceous chalk in the WNB is consistent with published compaction trend curves. This implies that the Late Cretaceous-mid Paleocene chalks in the southern part of the WNB presently are all at maximum depth of burial.
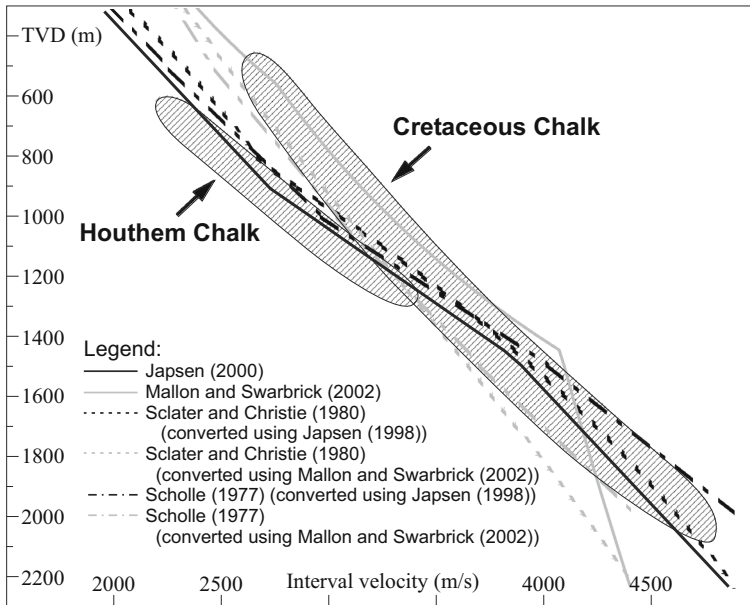
**Fig. 4** Comparison of the observed compaction trend of the Ommelanden and Houthem Chalk with those from published studies
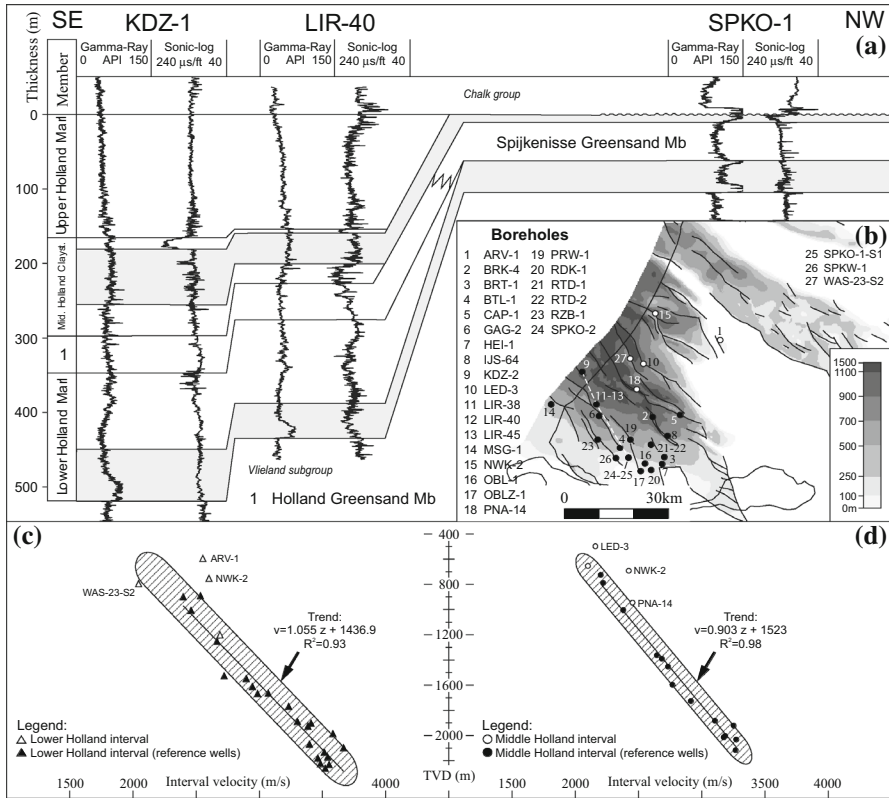
## 2.2 Holland formation

The Early Cretaceous Holland Formation (Upper Rijnland Group; Fig. 1) was deposited in an open marine environment. The three marl and claystone members defined within the formation have consistent lithology in the entire basin (Van Adrichem Boogaert and Kouwe 1997). The upper part of the formation in a large part of the basin is missing due to erosion (see Fig. 1).

Two intervals were selected for the analysis. The first interval consists of the lowermost ∼80–100 m of the Lower Holland Marl Member (see Fig. 5a; referred to as Lower Holland interval). In the marginal part of the basin, where the Lower Holland Marl Member is thin, the entire sequence was used for the analysis. The other interval used in the analysis is represented by the uppermost part of the Middle Holland Claystone Member (∼50 m thick; referred to as Middle Holland interval). Both intervals could be easily correlated in the basin using the characteristic log pattern.

To reliably define the baselines for the Lower- and Middle Holland intervals, reference data points with shallow depth are needed. The group of reference wells for the Holland Formation therefore was extended by wells where only a thin chalk layer is preserved, but no chalk anomaly was observed (see Fig. 5b).

The cloud of reference data points for the Middle Holland interval shows little scatter and defines a very reliable baseline (Fig. 5d). For the Lower Holland interval the quality is also good, although there is some scatter between 1800 and 2100 m caused by wells located at the margin of the basin (Fig. 5c). Probably the thin preservation and/or a slightly different lithology cause this. It is important to note that for both intervals the increase of velocity with depth is smaller than for the chalk (the baseline is steeper). Consequently,

**Fig. 5 a** Lithostratigraphy and characteristic log pattern of the Holland Formation. The investigated Lower- and Upper Holland intervals are indicated in *grey*. **b** Preserved thickness of the Early Cretaceous Rijnland Group. Boreholes indicated by *black circles* represent the reference wells, which were used to constrain the baselines. **c** Interval velocity-depth pairs for the Lower Holland interval. **d** Interval velocity-depth pairs for the Upper Holland interval

smaller burial anomalies are more difficult to recognise in the case of the Holland Formation.

For the Lower Holland interval two anomalies clearly separated from the reference points are observed (NWK-2 and ARV-1; Table 1). For the Middle Holland interval also two positive anomalies were found (NWK-2 and LED-3). Considering the tectonic position of the NWK-2, LED-3 and ARV-1 wells in the basin it is possible that these anomalies are caused by exhumation.

## 2.3 Vlieland claystone formation

The Vlieland Claystone Formation of Early Cretaceous age belongs to the Vlieland Sub-group of the Rijnland Group (see Fig. 1). The group was deposited in a shallow marine, near-shore environment (e.g., Den Hartog Jager 1996) and has a complex, laterally inhomogeneous structure with interfingered clay and sand bodies (Fig. 6a). Because of this it is difficult to find such a stratigraphic unit of uniform lithology, which can be easily correlated in the entire study area.

**Table 1** Results of the burial anomaly analysis and the geometrical approach (for map-view see Fig. 10)

| | | Burial anomaly analysis | | | | | | | | | Geom. Appr. | | Dir. Obs. | Decision |
|---|---|---|---|---|---|---|---|---|---|---|---|---|---|---|
| | Well name | BA HOUT | BA OMM | BA MH | BA LH | BA VL | BA AAL | BA SL | Cons. | Erosion | BA | Erosion | Uplift | Erosion |
| 1 | AND-6 | — | — | — | — | — | 100-450 | <150/WCRP | NO | <1340 | — | — | — | <900/MDB |
| 2 | ARV-1 | — | — | — | 325-475 | — | 150/WCRP | WCRP | NO | <1021 | — | — | — | 500-1100 |
| 3 | BAC-1 | — | — | — | — | — | WCRP/REF | WCRP/REF | YES | <948 | — | — | — | MDB |
| 4 | BHG-1 | — | WCRP/REF | — | — | — | — | — | YES | <896 | — | — | — | <300/MDB |
| 5 | BRK-4 | — | WCRP | — | WCRP/REF | WCRP/REF | — | — | YES | <460 | MDB | — | — | <300/MDB |
| 6 | BRK-5 | — | WCRP | — | — | — | — | — | | | | | | |
| 7 | BRT-1 | WCRP/REF | WCRP/REF | WCRP/REF | WCRP/REF | — | — | — | YES | <940 | — | — | — | <300/MDB |
| 8 | BTL-1 | WCRP/REF | WCRP/REF | WCRP/REF | WCRP/REF | — | — | — | YES | <1083 | MDB | — | — | <300/MDB |
| 9 | BUM-1 | — | — | — | — | — | 200-450 | 350-550 | YES | 1100-1400 | — | — | — | 1100-1400 |
| 10 | CAP-1 | WCRP | WCRP | WCRP/REF | WCRP/REF | WCRP/REF | WCRP/REF | — | YES | <426 | — | — | — | <300/MDB |
| 11 | EHV-1 | <100/REF | WCRP/REF | — | — | — | — | — | YES | <854 | — | — | — | <300/MDB |
| 12 | EVD-1 | — | — | — | — | — | 450-700 | 325-525 | YES | 1200-1500 | — | — | — | 1200-1500 |
| 13 | GAG-1 | <80/REF | WCRP/REF | — | — | — | WCRP/REF | — | YES | <880 | MDB | — | — | <300/MDB |
| 14 | GAG-2 | WCRP/REF | WCRP/REF | WCRP/REF | WCRP/REF | WCRP/REF | — | — | | | | | | |
| 15 | HEI-1 | WCRP/REF | WCRP/REF | WCRP/REF | WCRP/REF | -300/REF | — | — | YES | <1024 | — | — | — | <300/MDB |
| 16 | HST-2 | — | — | — | — | — | 100-400 | 0-200 | YES | 800-1000 | — | — | — | 800-1000 |
| 17 | HST-2-S1 | — | — | — | — | — | 300-600 | 250-450 | | | | | | |
| 18 | HVS-1 | WCRP/REF | WCRP/REF | — | — | — | — | — | YES | <1157 | MDB | — | — | <300/MDB |
| 19 | IJS-64 | — | WCRP | WCRP/REF | WCRP/REF | — | — | — | YES | <550 | — | — | — | <300/MDB |
| 20 | IJS-65 | — | WCRP | — | — | — | — | — | | | | | | |
| 21 | JUT-1 | — | — | — | — | — | 50-300 | 100-300 | YES | 1000-1200 | — | — | >1510 | 1500-1600 |
| 22 | KDZ-2 | — | 100-250/REF | WCRP/REF | WCRP/REF | <200/REF | WCRP/REF | -750/REF | NO | <645 | MDB | 152 | — | <300/MDB |
| 23 | KWK-1 | — | — | — | — | — | WCRP | WCRP | YES | <1146 | — | — | — | MDB |
| 24 | LED-1/2 | — | — | — | — | — | — | — | — | — | 147 | 578 | — | ~600 |
| 25 | LED-3 | — | — | 125-225 | — | — | — | — | YES | 575-675 | 220 | 667 | — | ~600 |
| 26 | LIR-38 | — | — | — | WCRP/REF | WCRP/REF | — | — | | | | | | |
| 27 | LIR-40 | — | WCRP/REF | WCRP/REF | WCRP/REF | WCRP/REF | — | -700/REF | YES | <730 | MDB | — | — | <300/MDB |
| 28 | LIR-45 | WCRP/REF | WCRP/REF | WCRP/REF | WCRP/REF | WCRP/REF | WCRP/REF | WCRP/REF | | | | | | |
| 29 | MID-101 | — | — | — | — | — | WCRP/REF | WCRP/REF | | | | | | |
| 30 | MID-102 | — | — | — | — | — | WCRP/REF | WCRP/REF | | | | | | |
| 31 | MID-103 | — | — | — | — | — | — | WCRP/REF | YES | <1150 | — | — | — | MDB |
| 32 | MID-201 | — | — | — | — | — | WCRP/REF | 800/REF | | | | | | |
| 33 | MID-301 | — | — | — | — | — | WCRP/REF | WCRP/REF | | | | | | |
| 34 | MKP-14 | — | — | — | — | WCRP | 75-375 | — | NO | 485-860 | 440 | 892 | — | 600-900 |
| 35 | MOL-2 | — | — | — | — | — | WCRP | — | YES | <671 | — | — | — | MDB |
| 36 | MON-2 | — | WCRP/REF | — | — | — | WCRP/REF | — | YES | <681 | MDB | — | — | <300/MDB |
| 37 | MRK-1 | — | — | — | — | — | 0-300 | — | YES | 700-1000 | — | — | — | 700-1000 |
| 38 | MSG-1 | — | — | WCRP/REF | WCRP/REF | — | WCRP/REF | — | YES | <1095 | MDB | — | >300 | <300/MDB |
| 39 | MSV-1 | WCRP/REF | WCRP/REF | — | — | — | — | — | YES | <1148 | MDB | — | — | <300/MDB |
| 40 | NWK-2 | — | — | 200-350 | 225-375 | 0-150 | 175-475 | — | YES | 660-810 | 264 | 710 | >580 | 700-800 |
| 40 | NWK-2* | — | — | — | — | — | WCRP | WCRP | | | | | | |
| 41 | OBL-1 | WCRP/REF | WCRP/REF | — | WCRP/REF | — | — | — | YES | <1054 | — | — | — | <300/MDB |
| 42 | OBLZ-1 | WCRP/REF | WCRP/REF | WCRP/REF | WCRP/REF | — | WCRP/REF | WCRP/REF | YES | <1122 | — | — | — | <300/MDB |
| 43 | OEG-1 | — | — | — | — | — | — | — | — | — | 214 | 722 | — | ~700 |
| 44 | OTL-1 | — | — | — | — | — | WCRP | WCRP | YES | <628 | — | — | — | MDB |
| 45 | PKP-1 | — | — | — | — | — | 200-450 | 0-225 | YES | 700-900 | — | — | — | 700-900 |
| 46 | PNA-14 | — | — | <150 | WCRP | — | — | — | YES | <416 | MDB | 269 | — | <300/MDB |
| 47 | PRN-1 | WCRP/REF | WCRP/REF | — | — | — | — | — | YES | <845 | MDB | — | — | <300/MDB |
| 48 | PRW-1 | WCRP/REF | WCRP/REF | WCRP/REF | WCRP/REF | WCRP/REF | WCRP/REF | WCRP/REF | YES | <1000 | MDB | — | — | <300/MDB |
| 49 | PRW-2 | — | — | — | — | WCRP/REF | WCRP/REF | 300/REF | | | | | | |
| 50 | RDK-1 | WCRP/REF | WCRP/REF | — | WCRP/REF | — | WCRP/REF | WCRP/REF | YES | <1098 | — | — | — | <300/MDB |
| 51 | RKK-10-S1 | — | WCRP | — | — | — | — | — | YES | <622 | — | — | — | <300/MDB |
| 52 | RTD-1 | — | — | — | WCRP/REF | WCRP/REF | WCRP/REF | — | | | | | | |
| 53 | RTD-12 | 60-160/REF | WCRP/REF | — | — | — | — | — | YES | <840 | — | — | — | <300/MDB |
| 54 | RTD-2 | — | — | WCRP/REF | WCRP/REF | — | — | — | | | | | | |
| 55 | RTD-5 | — | WCRP/REF | — | — | — | — | — | | | | | | |
| 56 | RZB-1 | WCRP/REF | WCRP/REF | WCRP/REF | WCRP/REF | — | WCRP/REF | -700/REF | YES | <1064 | MDB | — | — | <300/MDB |
| 57 | SPKO-1-S1 | WCRP/REF | WCRP/REF | — | WCRP/REF | — | WCRP/REF | WCRP/REF | YES | <1150 | MDB | — | — | <300/MDB |
| 58 | SPKO-2 | — | WCRP/REF | — | WCRP/REF | — | — | — | | | | | | |
| 59 | SPKW-1 | WCRP/REF | WCRP/REF | — | WCRP/REF | — | WCRP/REF | WCRP/REF | YES | <1222 | MDB | — | — | <300/MDB |
| 60 | SPL-1 | — | — | — | — | — | 100-400 | 500-700 | YES | 800-1400 | — | — | >140 | 800-1400 |
| 61 | STW-1 | — | — | — | — | — | WCRP/REF | — | YES | <1085 | — | — | — | <300/MDB |
| 62 | WAA-1 | — | — | — | — | — | WCRP | WCRP | YES | <910 | — | — | — | MDB |
| 63 | WAS-23-S2 | — | — | WCRP | -150 | ~150/WCRP | — | — | YES | 490-640 | 150 | 603 | — | ~600 |
| 64 | WAZ-1 | — | — | — | — | — | — | — | — | — | MDB | 441 | >436 | ~450 |
| 65 | WLK-1 | — | — | — | — | — | 750-1050 | 700-900 | YES | 1400-1700 | — | — | — | 1400-1700 |
| 66 | WOB-1 | — | — | — | — | WCRP | ~200/WCRP | WCRP | YES | 430-630 | ~300 | ~730 | — | ~500-600 |
| 67 | WRV-1 | — | — | — | — | — | WCRP/REF | WCRP/REF | YES | <569 | — | — | — | <300/MDB |
| 68 | WSP-1 | — | — | — | — | — | 0-250 | 75-275 | YES | 880-1130 | — | — | — | 900-1100 |

NWK-2* indicates the autochton part of the NWK-2 well below a major thrust fault

*BA* amount of burial anomaly, *HOUT* Houthem Chalk, *OMM* Ommelanden Fm., *MH* middle Holland interval, *LH* lower Holland interval, *VL* upper Vlieland interval, *AAL* Aalburg Fm., *SL* Sleen Fm., *Cons.* consistency among the studied intervals regarding burial anomaly, *Geom. Appr.* geometrical approach, *Dir. Obs.* direct observation, *WCRP* *w*ithin *c*loud of *r*eference *p*oints (i.e., no burial anomaly), *REF* reference well used to constrain the baseline, *MDB* *m*aximum *d*epth of *b*urial (i.e., no burial anomaly). Values are in meters
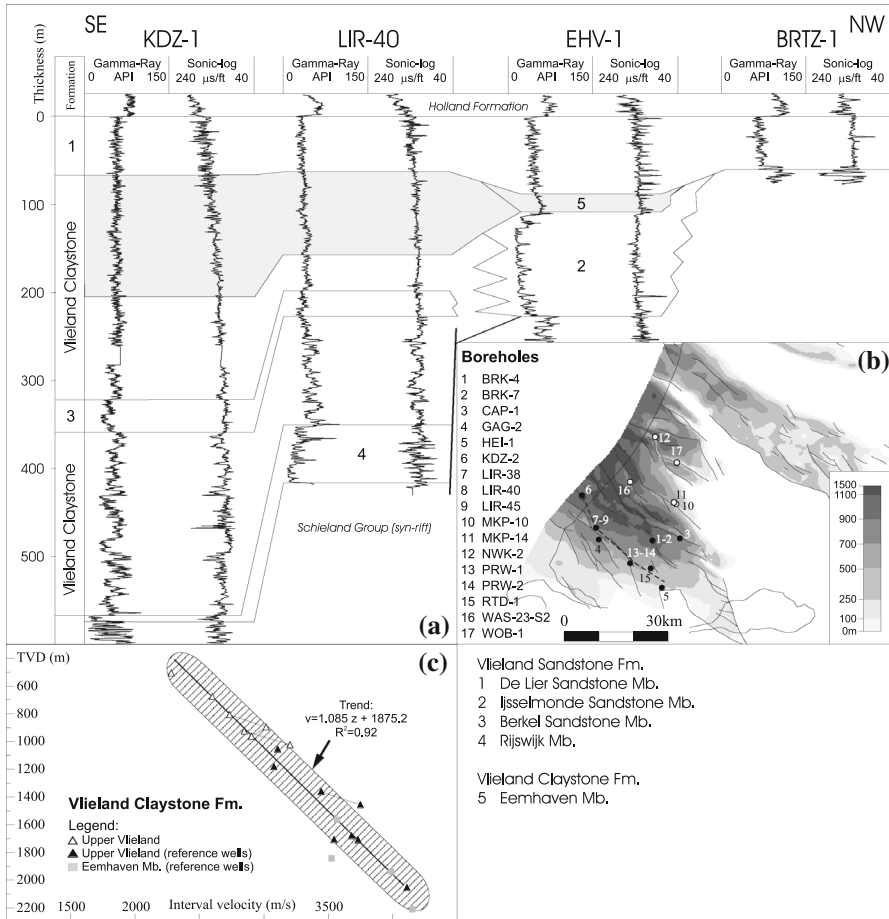
**Fig. 6** **a** Lithostratigraphy and characteristic log pattern of the Vlieland Subgroup of the Rijnland Group. The investigated interval is indicated in *grey*. **b** Preserved thickness of the Early Cretaceous Rijnland Group. Boreholes indicated by *black circles* represent the reference wells, which were used to constrain the baseline. **c** Interval velocity-depth pairs for the Upper Vlieland interval

For the present analysis the thick sandy clay deposits succeeding the Berkel Member of the Vlieland Sandstone Formation were used (referred to as Upper Vlieland; Fig. 6a). This interval is characterised by a relatively "calm" sonic log response compared to the succession below the Berkel Member. The lack of characteristic log patterns, however, did not allow for further subdivision. For the analysis therefore, one or more ∼50–100 m thick intervals were selected, whose sonic log indicated consistent seismic velocities. For wells located in a marginal position the Eemhaven member of the formation was used (Fig. 6a).

Below 1300 m the reference data points show some scatter, which is partly due to the thin Eemhaven member (Fig. 6c). The figure reveals on the other hand that the linear trend determined by the reference points coincides remarkably well with the shallow data points, where a burial anomaly would be expected. None of these wells shows a clear separation from the reference cloud.

## 2.4 Lower Jurassic clays (Sleen and Aalburg formations)

In the Early Jurassic open marine environments dominated the area of the WNB, in which a thick clay succession with occasional limestone beds was deposited. The Sleen and the Aalburg Formations represent the lowermost part of this succession, which displays pronounced differences in thickness as a result of syn-sedimentary faulting (e.g., Worum et al. 2004; Fig. 7b). Both of these formations are widespread in the WNB, but they are missing, or significantly reduced in thickness outside the basin centre. Three intervals, defined in 41 wells, were selected for the analysis: the entire Sleen Formation (only ∼30–50 m thick) and two intervals from the Aalburg formation (referred to as Lower- and Upper Aalburg intervals; Fig. 7a). The log characteristics of the Lower Aalburg interval do not suggest uniform, homogeneous lithology. The definition of this interval, however, was necessary, since without it there would not have been enough data points to constrain the amount of erosion in the eastern part of the basin. In wells where the formation is very thick, an additional 100–150 m thick interval from the upper part of the Aalburg Formation was also studied. The lack of characteristic log patterns however, did not allow correlating these intervals precisely between the wells.

Compared to the reference points of the younger formations discussed above, the reference points for the lower Jurassic intervals do not cover a large depth range. This makes the
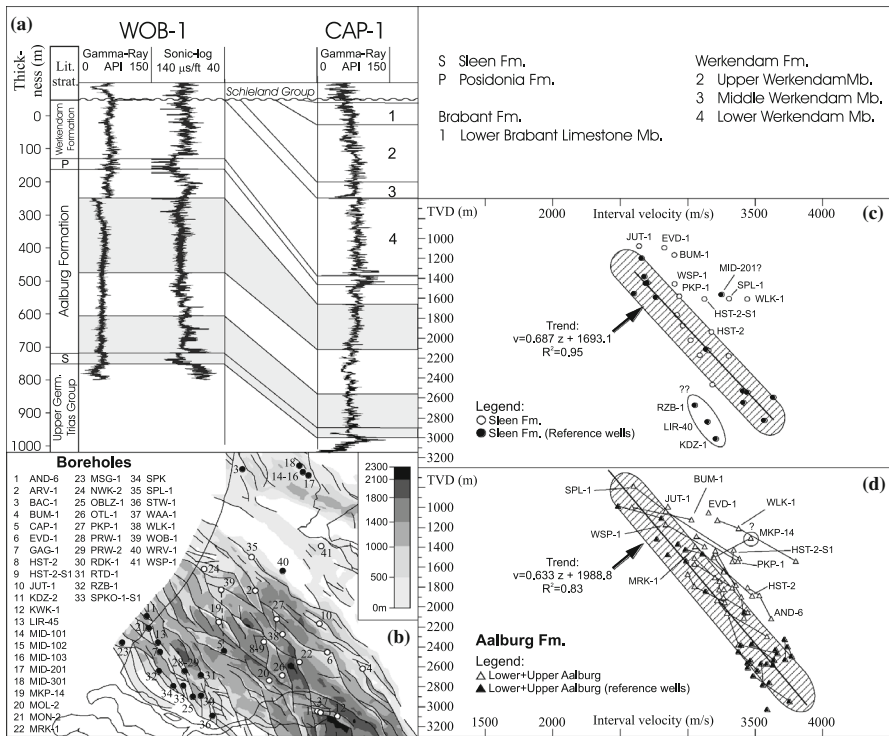


**Fig. 7** **a** Lithostratigraphy and characteristic log pattern of the Early Jurassic Altena Group. The investigated intervals (Sleen, Lower- and Upper Aalburg) are indicated in *grey*. **b** Preserved thickness of the Altena Group. Boreholes indicated by *black circles* represent the reference wells, which were used to constrain the baselines. **c** Interval velocity-depth pairs for the Sleen Formation. **d** Interval velocity-depth pairs for the Aalburg Formation

definition of the baseline difficult. For this reason additional wells located north of the basin (Zandvoort Ridge (WRV-1 well) and in the NW part of the Central Netherlands Basin (BAC-1 and MID-wells)) were added to the reference wells (Fig. 7b). In these wells erosion is suggested to be either small and/or masked by the significant Cenozoic sedimentation.

### 2.4.1 Sleen formation

For the Sleen Formation the RZB-1, the LIR-40 and the KDZ-2 wells show significantly lower interval velocity than the rest of the reference wells (Fig. 7c; see Sect. 4 at the Aalburg Formation below), while well MID-201—despite being a reference well—shows anomalously high interval velocity. These four wells were excluded from the definition of the baseline. Outside the cloud of reference points nine anomalies were found (see Table 1), the locations of which coincide with a major hiatus in the sedimentary record. It is suggested therefore that these deviations represent true burial anomalies related to erosion.

### 2.4.2 Aalburg formation

The reference points for the Lower and Upper Aalburg intervals define almost the same baseline, so it was decided to merge the two data sets (Fig. 7d). This has two major advantages: (1) the definition of the baseline is based on a larger, combined data set; (2) each well contains more (two or three) data points, consistency of which provides constraints on the quality and reliability of the burial anomaly. In an ideal case the line connecting the data points of a given well (intra-well compaction trend) should be parallel to the baseline defined by the reference wells ("global" compaction trend). This kind of consistency of the data points allows identifying those true burial anomalies, which do not separate unequivocally from the cloud of reference points.

As for the Sleen Formation the baseline for the Aalburg formation is also very steep. In addition, the cloud of reference points is wider than for the other studied intervals (i.e., the reference data set is "noisier"). Inconsistencies are most significant below 2300 m, which is also manifested in the intra-well compaction trends in this depth being not parallel to the "global" baseline. Presently, the pressure of the pore fluid in the Aalburg formation, which contains several hydrocarbon-prone bituminous layers (Bodenhausen and Ott 1981), is hydrostatic. In the past however, during for example the Late Jurassic-Early Cretaceous period of strong subsidence or during the expulsion of hydrocarbons, overpressure might have developed within the thick clayey succession. This could have caused abnormal compaction of the formation. In addition, Beekman et al. (2000) showed that mechanically weak clay layers tend to experience significant plastic deformation during inversion. Considering that the formation is relatively uniform lithologically, it is suggested that external factors such as those mentioned above could play an important role in the scatter of the sonic velocities of the reference wells.

Clear burial anomalies are identified in ten wells, which are located in the significantly eroded northern and north-eastern part of the basin (Figs. 1, 7b). These anomalies are suggested to be erosion-related. The anomalies for wells MRK-1 and WSP-1 do not separate clearly from reference points. The position of these wells however suggests that these anomalies although being small ($\sim$200–300 m) are related to erosion. When determining the burial anomaly in well MKP-14 the shallowest data point was not taken into account, since it is not consistent with the other two data points and with the baseline. For well NWK-2 the uppermost interval investigated within the Aalburg Formation is separated by a

major thrust fault from the two other intervals. The interval velocity-depth points from the deeper intervals (footwall) are located within the cloud of reference points, while the third data point (hangingwall) shows a clear anomaly (Table 1). This suggests that uplift and erosion in this well is related to a local phenomenon (uplift of the hanging-wall block of a reverse fault) rather than to the regional uplift of the area (see further discussion later).

## 3 Geometric reconstruction of the amount of erosion

Before discussing the results of the burial anomaly analysis another approach is presented, which aims to determine the pattern of erosion using the geometry of interpreted 3-D seismic horizons. This approach is complementary to the burial anomaly analysis and on a local scale should provide comparable results. The combination of these methods provides better constraints on the erosion pattern in the basin. The geometric restoration of the erosion was performed only in the western part of the basin where from a lithostratigraphic point of view only few units are missing (i.e., the Chalk Group and the upper part of the Rijnland Group; Fig. 1), and where good quality 3-D seismic surveys are present. The reconstruction is performed in four steps (Fig. 8a).

Step 1    The first step is to restore the base Chalk Group horizon in areas of the basin where it is not preserved (Fig. 8a). This restored horizon is referred to as fictional base Chalk Group horizon (FBCG). Where 3-D seismic surveys are available (central part of the basin) the FBCG horizon was interpreted on seismic sections using the geometrical characteristics of preserved reflectors within the Rijnland Group as guides (Fig. 8b). The principle behind this interpretation is the assumption that the pattern of the FBCG horizon is similar to the pattern of preserved reflectors within the Rijnland Group. This homogeneous character of deposition in the Rijnland Group was also described by DeVault and Jeremiah (2002) and Jeremiah et al. (2010). In other words, the position of the FBCG horizon—and therefore also the thickness pattern of the Rijnland Group—is estimated using the thickness pattern of preserved subunits observed on the seismic sections. The applicability of this procedure is justified by the excellent correlation observed between the total thickness of the un-eroded Rijnland Group and the thickness of the Vlieland subgroup within it (Fig. 8a). Interpretation of the FBCG horizon commenced from preserved patches of the Chalk Group, allowing for reliable interpretation across faults

Step 2    The second step of the reconstruction was the depth conversion of the FBCG horizon. For this a linear velocity model ($v = v_0 + K \cdot z$) was used with $v_0$ and $K$ parameters determined for the Rijnland Group (TNO-NITG 2002). As a quality control the depth converted FBCG horizon was compared with values calculated in the constraining wells (wells shown by open circles; Fig. 8a) using the estimated thickness of the Rijnland Group (constrained by the Rijnland Group-Vlieland Subgroup cross-plot) subtracted from the depth of the mapped base Rijnland Group horizon. The comparison revealed that the depth converted FBCG horizon systematically overestimated the depth obtained from the cross-plot method ($\sim$200 m in average). For this reason a depth correction map was constructed, which has a value of zero where the chalk is preserved and gradually increases towards the interior and eastern parts of the map. Correcting the depth converted FBCG horizon with this map does not change the general pattern (i.e.,
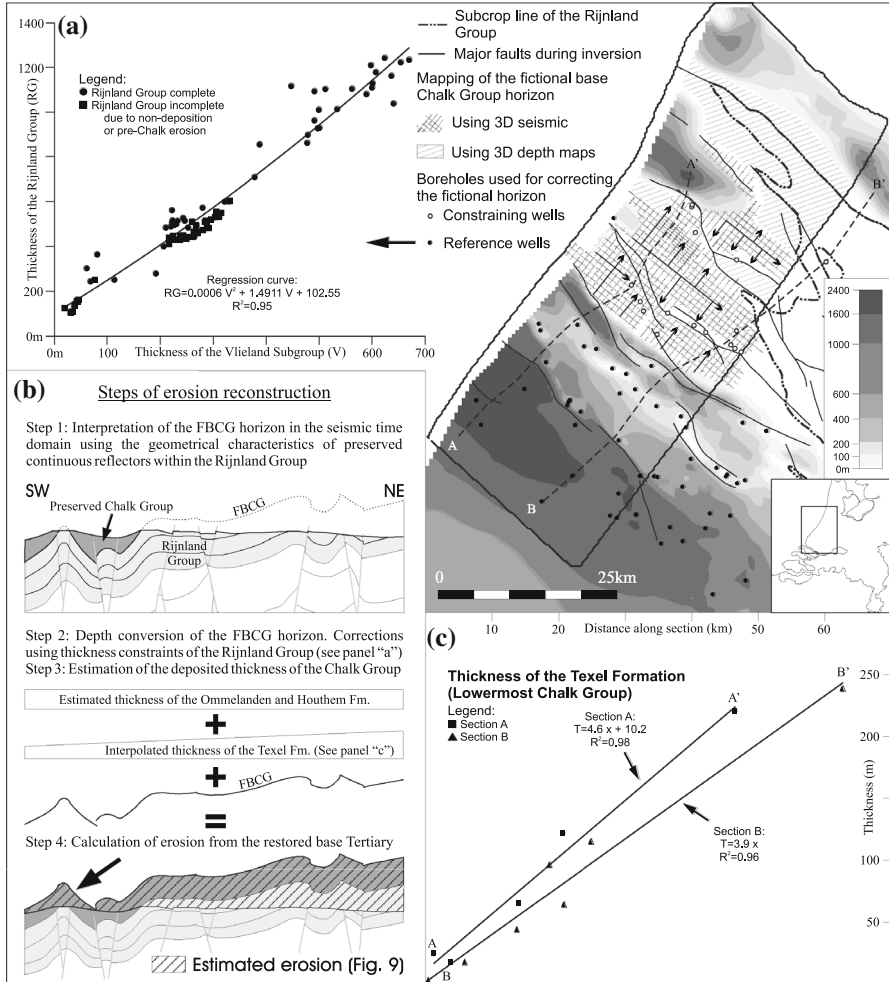
**Fig. 8** Geometric restoration of the amount of sediment eroded from the western part of the West Netherlands Basin. **a** Cross-plot between the thickness of the Vlieland Subgroup and the Rijnland Group. The map on the *right* shows the outline of the restored area. The *colour scale* shows the preserved thickness of the Chalk Group. **b** Main steps of the erosion reconstruction (see text for discussion). **c** Deposited thickness of the Texel Formation along sections A and B

shape) of the FBCG horizon. The corrected horizon satisfies the well data within the error range of the cross-plot. In the northern part of the map where there is no 3-D seismic coverage the FBCG horizon was determined using digitally available 3-D depth models and cross sections. The procedure is similar to that used in the seismic interpretation. Note that because of the lack of suitable data, in this area the FBCG horizon could not be constrained by the cross-plot method, therefore more uncertainty should be considered. At the end of the second step the base Chalk Group horizon was fully restored in the entire study area by merging the FBCG horizon and the preserved patches of the base Chalk Group horizon obtained using traditional mapping

*Step 3*  The third and most critical step of the erosion reconstruction involves estimation of the pre-erosion thickness of the Chalk Group: this consists of the determination of the deposited thickness of the Houthem and Ommelanden Formations as well as the thickness of the Texel Formation (lowermost Chalk Group). Regarding the Texel Formation borehole data indicate a gradually increasing thickness towards the N-NNE (Fig. 8c), based on which a thickness map was constructed Estimation of the deposited thickness of the Ommelanden Formation is very difficult, since its deposition was coeval with the first phase of basin inversion (Late Santonian-Mid Campanian; Baldschuhn et al. 1991; Gras and Geluk 1999). Indirect evidence from the WNB and neighbouring Roer Valley Graben (RVG) was used to constrain the thickness of this formation. As demonstrated by the sonic velocity data (see earlier), the chalk presently is at maximum depth of burial, which indirectly indicates that the total deposited thickness of the Ommelanden Formation in the central part of the basin was definitely less than ∼500 m (based on BRK- and CAP-1 wells). This thickness is less than the amount preserved in the marginal chalk depocentres north and south of the WNB and RVG (i.e., Voorne Trough, South Limburg, Peel Block, Maasbommel High; Fig. 1). Gras and Geluk (1999) showed that the thickest Late Cretaceous succession on the Maasbommel High is coeval with the basin inversion and it is originated from the uplifting and eroding RVG. In contrast to the Roer Valley area, the syn-inversion sediments on the southern flanks of the WNB are not siliciclastic (TNO-NITG 2002), suggesting that during the first phase of inversion erosion (if it occurred) was not large enough to truncate down to the Early Cretaceous and older siliciclastic sediments. In fact, considering the continuously rising sea level during the first phase of basin inversion (Haq et al. 1987), it is speculated that in the WNB, the sea level rise could keep up with the inversion-related tectonic uplift of the basin, therefore non-deposition rather that erosion characterised the first phase of inversion. As Gras and Geluk (1999) demonstrated in the RVG, sediment deposition in the central, inverted part of the basin resumed only when the inversion movements abated at the end of the Cretaceous. This is assumed to be valid also in the WNB Following from the above it is suggested that the main erosional phase in the WNB occurred during the second phase of inversion (Mid Paleocene), which was accompanied by a major drop in global sea level (Haq et al. 1987). During the Late Cretaceous inversion phase non-deposition was more likely. Consequently, the amount of deposited chalk in the centre of the basin roughly can be estimated by summing the thickness of the pre-Campanian chalk and Maastrichtian-Danian chalk, which is ∼100 + 200 = 300 m (based on Fig. 3a). Note that this amount (1) is only a rough estimate, since precise chronostratigraphic markers are not available and (2) is only valid in the centre of the basin. In the Voorne Trough and in inversion-related synclines where sedimentation was most probably continuous during the first phase of inversion the thickness of the deposited chalk is (much) larger (see Fig. 3a)

*Step 4*  During the last step of the erosion reconstruction the amount of eroded sediments are calculated. This is equal to the difference between the present-day base Tertiary horizon and a horizon calculated by adding the estimated thickness of the Chalk Group to the restored base Chalk Group horizon (Fig. 8b). The thickness of the Chalk Group is estimated by the sum of the 2-D grid representing the Texel Formation and a uniform thickness of 300 m representing the Ommelanden and Houthem Formations

## 4 Discussion

In the following the map of the geometrically restored erosion (Fig. 9) and the results of the burial anomaly analysis are evaluated. First the pattern and the magnitudes of erosion are studied, followed by a discussion on the implications of the results for hydrocarbon maturation.

### 4.1 Pattern of erosion

It is important to note that the pattern of erosion determined using the geometric approach presented above greatly depends on the assumed thickness of the Ommelanden and Houthem Formations. Syn-tectonic redeposition and mass transfer of chalk sediments on the flanks of the basin likely occurred during the first phase of inversion, which provides an obstacle for the correct 3-D erosion reconstruction. However, in the central, uplifting part of the WNB, where redeposition-related excess chalk sediments were likely not present, it is reasonable to assume that a chalk layer of relatively uniform thickness was deposited. Therefore, in this part of the basin the pattern of removed sediments determined by the geometrical approach is valid even if the magnitude of the deposited Late Cretaceous chalk was estimated incorrectly. It should be emphasised however, that in the south-western part of Fig. 9a (Voorne Trough) the amount of originally deposited chalk and consequently the amount of erosion is underestimated.

Analysis of Fig. 9a reveals that the pattern of erosion varies significantly laterally and has a high frequency local and a low frequency regional component. The regional component shows a general increase of erosion towards the East. This is in agreement with the observed subcrop pattern below the base Tertiary horizon (Fig. 1). The eastward increasing erosion suggests a regional, dome-like uplift of the WNB, which reached its maximum in the eastern part of the basin. The local, high frequency pattern of erosion is superimposed onto the regional trend and is fault-related (Fig. 9). The maximum of local erosion is associated either with strongly tilted fault blocks (e.g., northern boundary fault of the WNB) or with the axis of fault-related anticlines (fault propagation folds and fault-drag folds). The faults involved in the folding are steep normal faults, which were reactivated in a reverse manner (Fig. 9c–d). The local minima of erosion are generally associated with elongated "erosional shelters", which are bounded on both sides by uplifted and/or folded areas. These elongated zones of minimum erosion generally form synclines deformed to varying degrees (Fig. 9c, d), and likely are locations of syn-inversion sedimentation during the Late Cretaceous.

### 4.2 Magnitude of erosion

The results of the burial anomaly analysis and the geometrical approach are summarised in Table 1. The burial anomaly-based erosion was calculated using Eq. (1). Direct observations regarding the amount of uplift in five wells are also listed. These wells penetrate duplications of part of the sedimentary succession separated by major thrust faults. The depth difference between the same stratigraphic horizon below and above the thrust fault estimates the minimum uplift of the hangingwall block in the given well. This process is also described for well JUT-01 in Nelskamp et al. (2008) where similar erosion values were estimated using maturity modelling calibrated to temperature and vitrinite reflectance.
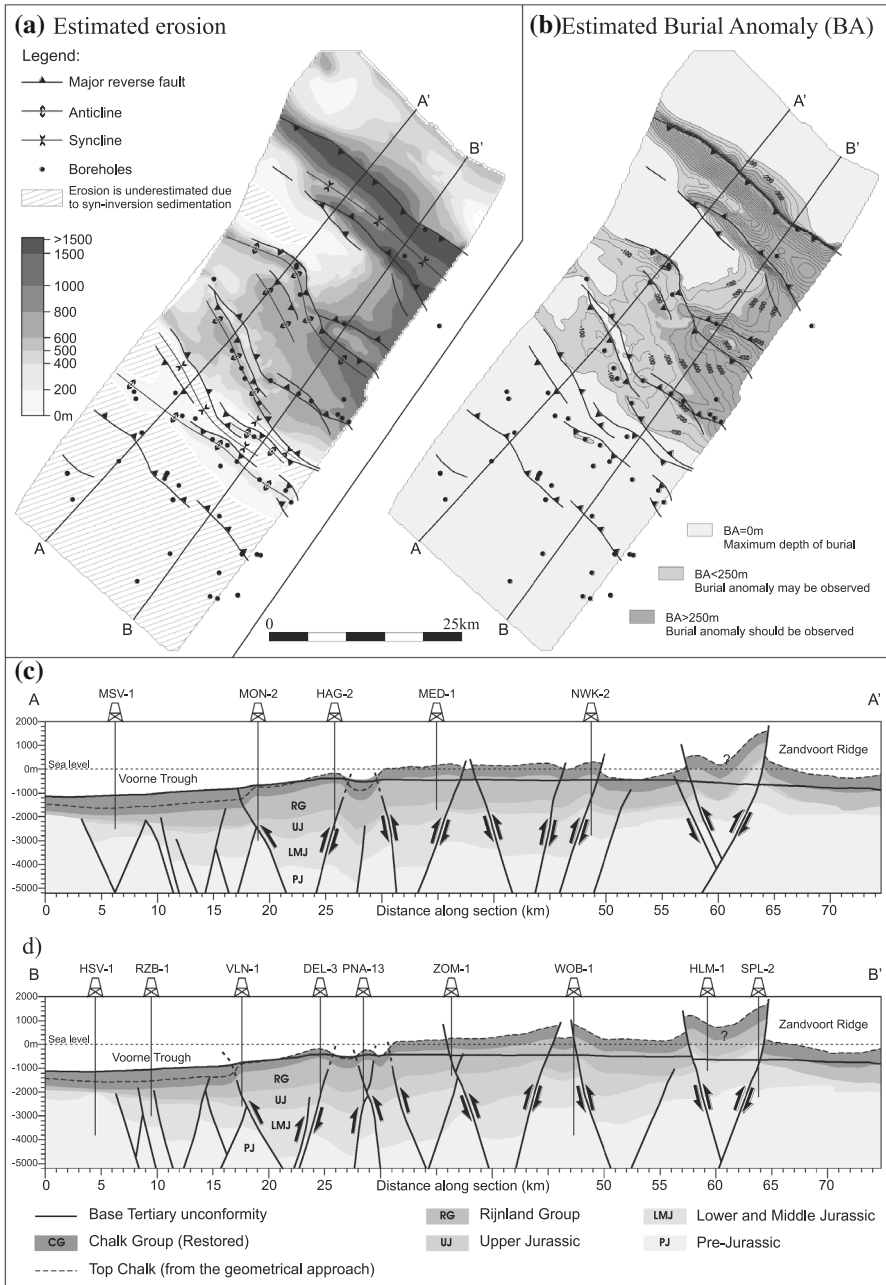
**Fig. 9** **a** Amount of erosion and **b** burial anomaly estimated using the geometrical approach. For outline of the maps see Fig. 8a. Note that erosion is underestimated in the south-western part of the map (see text for discussion) **c**, **d** Geological cross sections across the restored area

The table reveals that except for four wells the burial anomalies of the various intervals are consistent with each other (see the column "consistency"). This indicates that the calculated erosion is reliable. The results show that in all wells where the Chalk Group is preserved, the measured sonic velocities of the studied intervals coincide with the normal compaction trends determined by the reference wells. Furthermore, as shown earlier the baseline determined for the Cretaceous chalk coincides also with published baselines. These results imply that the Late Cretaceous-Mid Paleocene chalks as well as underlying sediments in the south-western part of the WNB are presently at their maximum depth of burial. The amount of erosion therefore cannot be determined precisely. It is estimated that the line, south of which the formations presently are at their maximum depth of burial, coincides approximately with the northern limit of the preserved Chalk Group (Fig. 10). The results of the geometric approach approximate the same boundary (Fig. 9b).

Wells CAP-1, BRK-4, BRK-5, IJS-64, IJS-65, PNA-14 and RKK-10-S1, in which the Chalk Group is significantly eroded bring important constraints on the Late Cretaceous tectono-sedimentological setting of the WNB. On one hand in these wells—although they do not show burial anomalies—the amount of erosion can be better constrained, since the post-erosion sedimentation is smaller than in wells located in the Voorne Trough. The lack of burial anomaly in these wells indicates a relatively small amount of erosion (smaller than ∼450 m) compared to other parts of the basin. On the other hand, since a certain amount of the Ommelanden chalk is still preserved in these wells, they imply that the maximum thickness of Late Cretaceous chalk deposited in the centre of the basin is much smaller than in the Voorne Trough. This suggests that continuous, syn-inversion sedimentation took place in the Voorne Trough while non-deposition or slight erosion characterised the central part of the WNB during the first phase of basin inversion in the Late Cretaceous. In the centre of the basin large thickness of chalk deposition, which was later removed by erosion, is not supported by the results of this study.
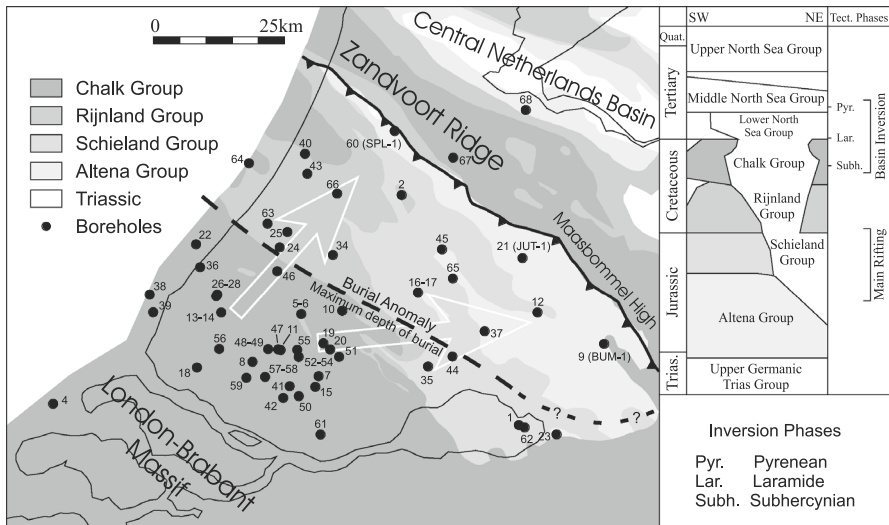


Fig. 10 General pattern of erosion in the West Netherlands Basin (for data see Table 1). Well numbers are the same as in Table 1. Background map represents the pre-Tertiary outcrop pattern. *White arrows* indicate the direction of increasing erosion

The geometrical approach presented earlier is independent from the burial anomaly analysis. The two approaches therefore should provide consistent results. Comparison of the erosion estimates indicates reasonably good (WOB-1, MKP-14 and WAS-23-S2 wells) and excellent (LED-3, NWK-2 and PNA-14) agreement between the two approaches (Table 1). In case of NWK-2 and WAZ-1 wells the results of the geometrical approach are in very good agreement also with direct observations, which estimate the minimum amount of uplift due to thrust faulting. This excellent correlation between different methods indicates that assuming 300 m of sedimentary cover during the Late Cretaceous-Mid Paleocene in the central part of the basin was a reasonable assumption. A larger amount of burial would lead to disagreement with the observed burial anomalies.

It is worthwhile to note that in wells JUT-1, BUM-1 and SPL-1 the observed burial anomaly is smaller in the upper part than in the lower part of the succession (Aalburg and Sleen Fm.). In addition in case of JUT-1 the erosion estimated using the amount of observed burial anomaly is smaller than the uplift calculated from the duplicated sedimentary succession. All of these wells are located close to the northern boundary fault of the WNB (see Fig. 10), along which significant reverse faulting and block rotation occurred during the inversion of the basin (Fig. 9c–d). It is suggested that in these wells the observed differences between the burial anomaly of the lower and upper parts of the Jurassic succession are the result of the syn-inversion rotation/deformation of the hangingwall block. Namely, if the hanging wall block rotates during thrust faulting, then the uplift of the lower part of the succession is larger than in the upper part, which is closer to the pole of the rotation.

In the last column of Table 1 the results of the various approaches are compiled. In the final estimated erosion not only the results of the various approaches but also local geological considerations, structural trends and results from nearby wells were taken into account. In case of BAC-1, MID-, OTL-1, MOL-2 and KWK-1 wells the burial anomalies were destroyed by the post-erosion sedimentation, and therefore the amount of erosion in these wells could not be estimated.

The compiled results indicate that the amount of erosion increases towards the east and northeast (Fig. 10). This can be seen also on the map of erosion constructed using the geometrical approach (Fig. 9a) and is in agreement with the subcrop pattern below the base Tertiary horizon. The erosion is highest in the eastern part of the basin especially along the main, north-eastern boundary fault (1100–1700 m; EVD-1, JUT-1, WLK-1 and BUM-1 wells). In this sense the inversion of the WNB can be considered as being asymmetric. A similar pattern was also observed in the Roer Valley Graben, the south-eastern continuation of the West Netherlands Basin. Here studies suggest a maximum of 1200 m of erosion along the north eastern boundary fault (Luijendijk et al. 2011). The amount of estimated maximum erosion is smaller than that determined for the neighbouring Broad Fourteens Basin, where 3000–3500 m of maximum erosion was suggested to have occurred along the central anticline of the basin (Nalpas et al. 1995, Abdul Fattah et al. 2012). In the south-eastern part of the WNB (AND-6, WAA-1, KWK-1) larger amount of erosion is expected than in the north-western part. This however, cannot be confirmed, since the burial anomalies were destroyed by the large Oligocene-present day subsidence of the Roer Valley Graben.

In the WNB, the Cretaceous and Tertiary is a major phase of maturation, expulsion and migration of oil from the Early Jurassic Posidonia shale source rock (e.g., De Jager et al. 1996; Van Balen et al. 2000). Nelskamp et al. (2012) and more recent work of Bruns et al. (2016), presents an extensive analysis of the thermal and maturity evolution for shale gas

potential the Netherlands, including the WNB. The latter study incorporated the erosion estimates presented in this paper.

## 4.3 Implications for geothermal exploration

Permeability of aquifers is a key parameter for geothermal doublet performance, as the flow performance of geothermal doublets scales approximately linearly with the product of aquifer permeability and thickness (e.g., Van Wees et al. 2012). In geothermal exploration for clastic aquifers, generally a linear relation is used between porosity of aquifers and the logarithm of permeability. Porosity has been determined in wells. In between wells, porosity needs to be spatially interpolated (Pluymaekers et al. 2012). Maximum burial depth should therefore be used in the spatial interpolation when adopting a porosity-depth curve or cokriging with maximum burial depth. The effects of burial anomaly (cf. Fig. 9a) result in a lowering of porosity up to 3%. Following the linear relationship between porosity and the logarithm of permeability observed in the geothermal aquifers in the Netherlands (Pluymaekers et al. 2012), Fig. 11 shows the effect of porosity anomalies of the WNB basin taking into account results from this study complemented with burial anomaly estimates from geometric reconstruction. The effects of porosity reduction clearly demonstrate up to a factor 3–4 reduction in permeability in the strongly inverted zones in the West Netherlands Basin. Consequently, the flow rates of geothermal doublets in these areas would be a few times lower with correction for burial anomaly than without. These findings clearly demonstrate the importance of taking burial anomalies into account and the added value of the workflow presented here to assess them correctly.
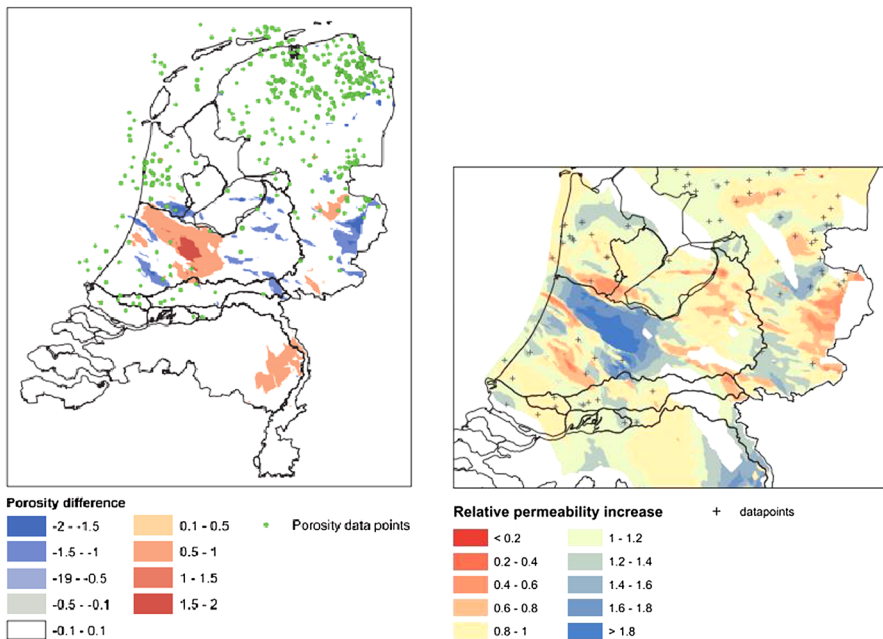


**Fig. 11** Predicted and permeability change taking into account burial anomalies (*left*) porosity change (*right*) permeability change. Porosity and permeability are constrained by well data (after Pluymaekers et al. 2012)

# 5 Conclusions

The study presented in this paper has shown that the pattern of exhumation in an inverted sedimentary basin can be reliably estimated if various methods are combined. By analysing the sonic log-based interval velocity patterns of properly defined stratigraphic intervals an erosion accuracy of 100–200 m can be obtained. Using the multi-formation approach the reliability of the estimated erosion can be further enhanced, provided consistency can be shown to exist between the results. Analysis of well-log based burial anomalies provides only local information about the amount of erosion, interpolation of which cannot provide a map reflecting the true pattern of erosion. The study has demonstrated however, that the geometrical approach involving the extrapolation of 3-D seismic reflectors constrained by the statistical relationship between the thicknesses of various lithostratigraphic units is a powerful tool to determine the detailed, high-resolution pattern of erosion in an inverted basin. The detailed map of erosion not only provides useful constraints on the inversion tectonics of the basin, but can also be used to better constrain its maturity history.

The results of this study indicate that in the West Netherlands Basin there are significant lateral variations in the pattern of erosion, which has a local, high frequency and a regional-, low frequency component. The regional component shows a general increase of erosion towards the east, which reaches its maximum along the north-eastern border fault of the basin. In a general sense this suggests asymmetric inversion of the West Netherlands Basin. Evidence from seismic sections and the high frequency component of the erosion suggest that reactivation of faults played a major role in the inversion and localised erosion of the basin fill. Across major faults several hundreds of meters of difference can be observed in the magnitude of erosion. The local maxima and minima of erosion are related respectively to fault-related anticlines and synclines.

Indirectly the results provide important constraints on the tectono-sedimentological aspects of the intra-chalk inversion phase (Late Santonian-Mid Campanian). This study suggests that the maximum thickness of the Late Cretaceous chalk in the centre of the basin at any moment during the Late Cretaceous is $\sim 300$ m. This amount is much smaller than the total preserved thickness of the Chalk in the Voorne Trough, indicating that continuous syn-inversion sedimentation was taking place in the Voorne Trough, while non-deposition or slight erosion characterised the centre of the inverting basin.

For geothermal exploration, burial anomalies can result in a pronounced reduction of permability in clastic aquifers, which results in up to a factor 5 reduction in the predicted flow performance of geothermal doublets.

# References

Abdul Fattah R, Verweij JM, Witmans N, Veen JT (2012) 4D Basin modelling of the Broad Fourteens Basin and offshore West Netherlands Basin; erosion and heat flow reconstruction and its influence on temperature, maturity and hydrocarbon generation. TNO public report TNO 2012 R10670: 168

Andriessen PAM (1995) Fission-track analysis; principles, methodology and implications for tectono-thermal histories of sedimentary basins, orogenic belts, and continental margins. Geol Mijnbouw 74(1):1–12

Anselmetti FS, Eberli GP (1993) Controls on sonic velocity in carbonates. Pure appl Geophys 141(2–4):287–323

Baldschuhn R, Best G, Kockel F (1991) Inversion tectonics in the north-west German basin. In: Spencer AM (ed) Generation, accumulation and production of Europe's hydrocarbons, Special Publication of the European Association of Petroleum Geoscientists, 1. Oxford University Press, Oxford, pp 149–159

Beekman F, Badsi M, Van Wees JD (2000) Faulting, fracturing and in situ stress prediction in the Ahnet Basin, Algeria—a finite element approach. Tectonophysics 320:311–329

Bodenhausen JWA, Ott WF (1981) Habitat of the Rijswijk oil province, onshore, The Netherlands. In: Illing
      LV, Hobson GD (eds) Petroleum geology of the continental shelf of NW Europe. Institute of Petro-
      leum, London, pp 301–309

Bouw L, Oude Essink GHP (2003) Fluid flow in the northern Broad Fourteens Basin during Late Cretaceous
      inversion. Neth J Geosci/Geologie en Mijnbouw 82(1):55–69

Bruns B, Littke R, Gasparik L, Van Wees JD, Nelskamp S (2016) Thermal evolution and shale gas potential
      estimation of the Wealden and Posidonia Shale in NW-Germany and the Netherlands: a 3D basin
      modelling study. Basin Res. doi:10.1111/bre.12096

Bulat J, Stoker SJ (1987) Uplift determination from interval velocity studies, UK southern North Sea. In:
      Brooks J, Glennie K (eds) Petroleum geology of North West Europe. Graham and Trotman, London,
      pp 293–305

Corcoran DV, Doré AG (2005) A review of techniques for the estimation of magnitude and timing of
      exhumation in offshore basins. Earth Sci Rev 72:129–168

Cornford C (1994) The Mandal-Ekofisk(!) petroleum system in the Central Graben of the North Sea. In:
      Magoon LB, Dow WG (eds) The petroleum system—from source to trap: AAPG Memoir 60,
      pp 537–571

De Jager J (2007) Geological development. In: Wong TE, Batjes DAJ, de Jager J (eds) Geology of the
      Netherlands. Royal Netherlands Academy of Arts and Science, pp 5–26

De Jager J, Doyle MA, Grantham PJ, Mabillard JE (1996) Hydrocarbon habitat of the West Netherlands
      Basin. In: Rondeel HE, Batjes DAJ, Nieuwenhuijs WH (eds) Geology of gas and oil under the
      Netherlands. Kluwer Academic Publishing, Dordrecht, pp 191–209

Den Hartog Jager DG (1996) Fluviomarine sequences in the Lower Cretaceous of the West Netherlands
      Basin: correlation and seismic expression. In: Rondeel HE, Batjes DAJ, Nieuwenhuijs WH (eds)
      Geology of gas and oil under the Netherlands. Kluwer Academic Publishing, Dordrecht, pp 229–241

DeVault B, Jeremiah J (2002) Tectonostratigraphy of the Nieuwerkerk Formation (Delfland subgroup), West
      Netherlands Basin. AAPG Bull 86(10):1679–1707

Dronkers AJ, Mrozek FJ (1991) Inverted basins of the Netherlands. First Break 9(9):409–425

Fabricius IL (2003) How burial diagenesis of chalk sediments controls sonic velocity and porosity. AAPG
      Bull 87(11):1755–1778

Gras R, Geluk MC (1999) Late Cretaceous-early tertiary sedimentation and tectonic inversion in the
      southern Netherlands. Geol Mijnbouw 78:1–19

Green PF, Duddy IR, Laslett GM, Hegarty KA, Gleadow AJW, Lovering JF (1989) Thermal annealing of
      fission tracks in apatite: 4. Quantitative modelling techniques and extension to geological timescales.
      Chem Geol Isot Geosci Sect 79(2):155–182

Hansen S (1996) A compaction trend for Cretaceous and Tertiary shales on the Norwegian shelf based on
      sonic transit times. Petrol Geosci 2:159–166

Haq BU, Hardenbol J, Vail PR (1987) Chronology of fluctuating sea levels since the Triassic. Science
      235:1156–1167

Heasler HP, Kharitonova NA (1996) Analysis of sonic well logs applied to erosion estimates in the Bighorn
      Basin, Wyoming. AAPG Bull 80(5):630–646

Hillis RR (1991) Chalk porosity and tertiary uplift, Western approaches trough, SW UK and NW French
      continental shelves. J Geol Soc Lond 148:669–679

Hillis RR (1993) Quantifying erosion in sedimentary basins from sonic velocities in shales and sandstones.
      Explor Geophys 24:561–566

Hillis RR, Thomson K, Underhill JR (1994) Quantification of tertiary erosion in the Inner Moray Firth using
      sonic velocity data from the chalk and the Kimmeridge clay. Mar Pet Geol 11(3):283–293

Japsen P (1993) Influence of lithology and Neogene uplift on seismic velocities in Denmark: implications
      for depth conversion of maps. AAPG Bull 77:194–211

Japsen P (1994) Retarded compaction due to overpressure deduced from a seismic velocity/depth conversion
      study in the Danish Central Trough, North Sea. Mar Pet Geol 11(6):715–733

Japsen P (1998) Regional velocity-depth anomalies, North Sea chalk; a record of overpressure and Neogene
      uplift and erosion. AAPG Bull 82(11):2031–2074

Japsen P (1999) Overpressured Cenozoic shale mapped from velocity anomalies relative to a baseline from
      marine shale, North Sea. Pet Geosci 5:321–336

Japsen P (2000) Investigation of multi-phase erosion using reconstructed shale trends based on sonic data;
      Sole Pit axis, North Sea. Glob Planet Change 24(3–4):189–210

Japsen P, Chalmers JA (2000) Neogene uplift and tectonics around the North Atlantic: overview. Glob
      Planet Change 24:165–173

Japsen P, Green PF, Nielsen LH, Rasmussen ES, Bidstrup T (2007) Mesozoic-Cenozoic exhumation events in the eastern North Sea Basin: a multi-disciplinary study based on palaeothermal, palaeoburial, stratigraphic and seismic data. Basin Res 19(4):451–490

Jeremiah JM, Duxbury S, Rawson P (2010) Lower Cretaceous of the southern North Sea Basins: reservoir distribution within a sequence stratigraphic framework. Neth J Geosci Geol Mijnbouw 89(3/4):203–237

Kenter JAM, Podladchikov FF, Reinders M, Van der Gaast SJ, Fouke BW, Sonnenfeld MD (1997) Parameters controlling sonic velocities in a mixed carbonate-siliciclastics Permian shelf-margin (upper San Andreas Formation, Last Chance Canyon, New Mexico). Geophysics 62(2):505–520

Luijendijk E, Van Balen RT, Ter Voorde M, Andriessen PAM (2011) Reconstructing the Late Cretaceous inversion of the Roer Valley Graben (southern Netherlands) using a new model that integrates burial and provenance history with fission track thermochronology. J Geophys Res 116:B06402

Magara K (1976) Thickness of removed sedimentary rocks, paleopore pressure, and paleotemperature, southwestern part of Western Canada basin. AAPG Bull 60:554–566

Mallon AJ, Swarbrick RE (2002) A compaction trend for non-reservoir North Sea Chalk. Mar Pet Geol 19(5):527–539

Mathiesen A, Bidstrup T, Christiansen FG (2000) Denudation and uplift history of the Jameson Land Basin, East Greenland—constrained from maturity and apatite fission track data. Glob Planet Change 24:275–301

Monsen K (2001) Acoustic velocity in fractured rock. J Geophys Res 106(B7):13261–13267

Moos D, Zoback MD (1983) In situ studies of velocity in fractured crystalline rocks. J Geophys Res 88(B3):2345–2358

Nalpas T, Le Douaran S, Brun JP, Unternehr P, Richert JP (1995) Inversion of the Broad Fourteens Basin (offshore Netherlands), a small-scale model investigation. Sed Geol 95:237–250

Nelskamp S, David P, Littke R (2008) A comparison of burial, maturity and temperature histories of selected wells from sedimentary basins in the Netherlands. Int J Earth Sci (Geol Rundsch) 97:931–953

Nelskamp S, Van Wees JD, Littke R (2012) Structural evolution, temperature, and maturity of sedimentary basins in the Netherlands: results of combined structural and thermal two-dimensional modeling. In Peters KE, Curry DJ, Kacewicz M (eds) Basin modeling: new horizons in research and applications: AAPG Hedberg Series, no 4, pp 137–156

Nyland B, Jensen LN, Skagen J, Skarpnes O, Vorren T (1992) Tertiary uplift and erosion in the Barents Sea: magnitude, timing and consequences. In: Larsen RM, Brekke H, Larsen BT, Talleraas E (eds) Structural and tectonic modelling and its application to petroleum geology. NPF Special Publication 1, Norwegian Petroleum Society (NPF), pp 153–162

Pluymaekers MPD, Kramers L, Van Wees JD, Kronimus RA, Nelskamp S, Boxem TAP, Bonté DDP (2012) Reservoir characterization of aquifers for direct heat production in mature oil and gas provinces: methodology and application to the Netherlands. Neth J Geosci 91–4:621–636

Poix O (1998) Sonic anomalies, a measure to quantifying overpressures. Overpressures in petroleum exploration; Proc Workshop, Pau, April 1998. Bull. Centre Rech Elf Explor Prod Mém 22:207–211

Racero-Baena A, Drake SJ (1996) Structural style and reservoir development in the West Netherlands oil province. In: Rondeel HE, Batjes DAJ, Nieuwenhuijs WH (eds) Geology of gas and oil under the Netherlands. Royal Geological and Mining Society of the Netherlands (KNGMG). Kluwer Academic Publisher, Dordrecht, The Netherlands, pp 211–227

Richardsen G, Vorren TO, Tørudbakken BO (1993) Post-Early Cretaceous uplift and erosion in the southern Barents Sea: a discussion based on analysis of seismic interval velocities. Nor Geol Tidsskr 73:3–20

Rohrman M, Van der Beek P, Andriessen P, Cloetingh S (1995) Meso-Cenozoic morphotectonic evolution of southern Norway: neogene domal uplift inferred from apatite fission track thermochronology. Tectonics 14:700–714

Scholle PA (1977) Chalk diagenesis and its relation to petroleum exploration; oil from chalks, a modern miracle? AAPG Bull 61:982–1009

Sclater JG, Christie PAF (1980) Continental stretching: an explanation of post-mid-Cretaceous subsidence of the central North Sea Basin. J Geophys Res 85(B7):3711–3739

Skagen JI (1992) Methodology applied to uplift and erosion. Nor Geol Tidsskr 72:307–311

Sweeney JJ, Burnham AK (1990) Evaluation of a simple model of vitrinite reflectance based on chemical kinetics. AAPG Bull 74:1559–1570

TNO-NITG (2002) Geological Atlas of the Subsurface of the Netherlands: explanation to mapsheets VII and VIII: Noordwijk-Rotterdam and Amsterdam-Gorinchem. Utrecht, 135 pp

Van Adrichem Boogaert HA, Kouwe WFP (1997) Stratigraphic nomenclature of the Netherlands, revision and update by RGD and NOGEPA. Mededelingen Rijks Geologische Dienst, Haarlem

Van Balen RT, Van Bergen F, de Leeuw C, Pagnier H, Simmelink H, Van Wees JD, Verweij JM (2000) Modelling the hydrocarbon generation and migration in the West Netherlands Basin, the Netherlands. Geologie en Mijnbouw/Neth J Geosci 79(1):29–44

Van Wees JD, Kronimus A, Van Putten M, Pluymaekers M, Mijnlieff H, Van Hooff Obdam A, Kramers L (2012) Geothermal aquifer performance assessment for direct heat production. Methodology and application to Rotliegend aquifers. Neth J Geosci 91–94, 651–665:54

Van Wijhe DH (1987) Structural evolution of inverted basins in the Dutch offshore. Tectonophysics 137:171–219

Vernik L, Nur A (1992) Petrophysical classification of siliciclastics for lithology and porosity prediction from seismic velocities. AAPG Bull 76:1295–1309

Verweij JM (2003) Fluid flow systems analysis on geological timescales in onshore and offshore Netherlands. Ph.D. Thesis, Netherlands Institute of Applied Geoscience TNO, Utrecht, The Netherlands, 278 p

Worum G, Michon L, Van Balen RT, Van Wees JD, Cloetingh SAPL, Pagnier HJM (2004) Pre-neogene controls on present-day fault activity in the West Netherlands Basin and Roer Valley Rift System (southern Netherlands): role of variations in fault orientation in a uniform low-stress regime. Quat Sci Rev Spec Publ 24:473–488

Ziegler PA (1990) Geological Atlas of Western and Central Europe, second and completely revised edition. Shell Int Pet Mij, The Hague